

## On the velocity, size and temperature of gaseous dendritic flames

Jorge Yanez,<sup>1</sup> Mike Kuznetsov,<sup>1</sup> and Fernando Veiga-López<sup>2</sup>

<sup>1</sup>Institute for Thermal Energy Technology and Safety, Karlsruhe Institute of Technology, Hermann-von-Helmholtz-Platz 1, 76344, Eggenstein-Leopoldshafen, Germany

<sup>2</sup>Fluid Mechanics Research Group, Universidad Carlos III de Madrid, Av. de la Universidad 30, 28911, Leganés (Madrid), España

(\*Electronic mail: jorge.yanez@kit.edu)

(Dated: 20 September 2022)

Dendritic combustion in Hele-Shaw cells is investigated qualitatively using a simplified one-dimensional thermo-diffusive model. Formulae for the velocity, size and temperature of the flamelets are derived. The temperature and velocity of the flames increase for small radii to allow for their survival regardless the activation energy. In addition, the results obtained with very large activation energy were compared with experimental results, finding that additional tests are required due to the strong influence of gravity on the velocity and size estimations. Conditions for the existence of this anomalous propagation are investigated, confirming analytically that it can only happen for low Lewis numbers.

### I. INTRODUCTION

Flames propagating in narrow gaps between two parallel plates (Hele-Shaw cell) show anomalous burning regimes for Peclet number below  $15^{1,2}$ . These regimes are characterized by the splitting of the continuous flame front into a set of flamelets separated by fresh unburned gas. Figure 1 shows two of the four flame propagation regimes identified in Yanez Escanciano et al.<sup>2</sup> which are of interest for this work: a) mono-cellular and b) bi-cellular flames propagating at an almost constant speed.

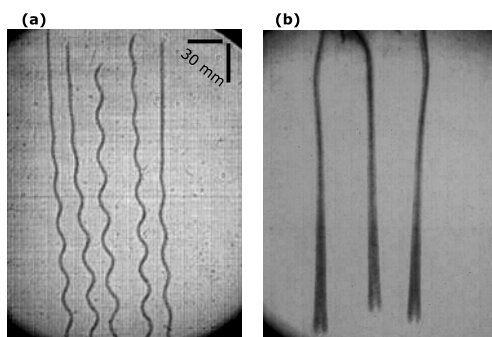


FIG. 1. Unconventional flame propagation categories of interest for this work: (a) mono-cellular and (b) bi-cellular. Taken from Veiga-López et al.<sup>1,3</sup>

In the numerical study exploring the experiments of Veiga-López et al.<sup>1</sup>, Martínez-Ruiz et al.<sup>4</sup> and Dominguez-Gonzalez et al.<sup>5</sup> were able to reproduce the mono- and bi-cellular cell patterns in a two-dimensional (2D) configuration. As in the work of Kagan and Sivashinsky<sup>6</sup>, the reported phenomena occurred only for low Lewis number mixtures,  $Le < 1$  and it was impossible to obtain for mixtures with  $Le \geq 1$ . The statistical exploitation of the data gathered by Veiga-López et al.<sup>1</sup>, carried out by Yanez Escanciano et al.<sup>2</sup>, confirmed that the Lewis number was required to be  $Le < 1$  to obtain unconven-

tional propagation. Nevertheless, it does not result to be the effect triggering the phenomenon. Instead, heat losses, characterized by Peclet number  $Pe$ , is the key to the flame splitting mechanism.

At this stage, one may just speculate regarding the potential applications of the phenomena. We foresee that it will have significant implications for safety because ultra lean hydrogen flames can propagate in more extended conditions than the community may initially have thought<sup>7</sup>.

The discovered regimes were novel for gaseous fuels<sup>1</sup>. Nevertheless, dendritic combustion patterns were observed initially for smoldering solid fuels in Hele-Shaw cells<sup>8-10</sup>. There, these authors linked the existence of the phenomena to the mass diffusivity of the deficient component, the comburent. The deficit of air was compensated by diffusion from surrounding areas creating a localized isolated zone of hotter combustion. This would counteract heat losses, keeping the hot spot above the limiting temperature and, therefore, sustaining the combustion process.

Dendritic combustion patterns were also observed in other configurations. Fingering in combustion of thick fuel plates was discovered by Matsuoka et al.<sup>11</sup> and Zhu et al.<sup>12</sup>. Similarly, dendritic patterns were detected utilizing a fuel consisting in a layer of aluminum particles lying inside of a Hele-Shaw cell<sup>13</sup>. Fingering combustion was also reported in microgravity experiments<sup>14</sup>. Notably, fingering was detected in an experiment that at normal gravity conditions did not exist.

In a theoretical study motivated by the phenomena detected by Zik et al.<sup>9</sup>, Kagan and Sivashinsky<sup>6</sup> created a model for the fingering pattern for solid fuels. Considering adiabatic conditions and performing asymptotic expansions, these authors derived a dispersion relation for the phenomena, thus providing a thorough analysis of the linear stability of such flames. Carrying out further simplifications, they were even able to deduce a weakly non-linear expression for the propagation of the flamelets. The expression is the well known Sivashinsky differential equation<sup>15</sup>. Note the striking analogy that due to this formulation is established between flame instabilities and the discontinuous flamelet regime. The integration of this equation by Kagan et al.<sup>6</sup> was notably able to describe the fragmented fronts appearing in the experiments, even re-

producing qualitatively, the splitting and joining of flamelets of the finger-like flame front. The diffusion of the limiting component was identified as the dominant factor of the process.

Dendritic combustion patterns also have an analogy with flame balls, as has already been recognized in<sup>4,16</sup>. In flame balls, the fuel of very lean hydrogen mixtures migrates to certain spots that effectively work as if there were higher fuel concentrations. This migration is due to the high diffusivity coefficient of the fuel, hydrogen. Being enriched with hydrogen, the hotter reaction zone is counterbalanced by heat losses in the form of radiation. Due to a deficit of fuel in the surroundings, a planar flame breaks up into fragments, which adopts spherical structures, hence providing the name of the regime. Such a mechanism is very similar to the one described by Zik et al.<sup>10</sup>. Although its existence was conjectured some years before, flameballs were originally observed by Ronney in microgravity, both in drop-tower experiments<sup>17</sup> and in spaceflights<sup>18</sup>. Recently, arrays of flameballs were even observed for hydrogen-methane blends at standard pressure conditions.

Flameballs were analyzed by Buckmaster and his coauthors in<sup>19-23</sup>. Originally, Buckmaster et al. analyzed a stationary flame without advection<sup>19</sup> utilizing volumetric heat losses. These authors described the quenching limits, and defined a radius domain for which such reactive structure resulted stable and thus could be observed. The original analysis was extended by Buckmaster et al.<sup>20</sup> to consider heat losses also in the unreacted mixtures, refining the stability domain. The hypothesis of advection free flow considered originally was subsequently abandoned in<sup>22</sup>, where also the effect of the Peclet number was analyzed. Theoretical results previously obtained were particularized for hydrogen-air mixtures by Buckmaster and Joulin<sup>21</sup>. In their numerical investigation, radiative heat losses were considered and the equivalence ratios for the existence of flameballs were obtained. Returning to the thermal diffusive model, Buckmaster et al.<sup>19</sup> analyzed the effect of conductive heat losses due to a neighboring wall on the stability domain. Although heat losses in the form of radiation seem to be inherent to the system,<sup>24</sup> it was shown that the regime is also possible, and stable, without losses.

All named authors analyzed a three-dimensional configuration that does not correspond to Hele-Shaw flows. Likewise, the previously summarized results of the classic analysis of Buckmaster and his co-workers cannot be applied to two or quasi two-dimensional configurations<sup>4</sup> as the boundary conditions cannot be fulfilled in a 2D configuration. Therefore, 2D flameballs were analyzed following an alternative formulation in Kagan et al.<sup>25</sup>. There, the effect of energy losses breaks up the flame and successive changes to the front topology were studied in a plane. In the limit of no expansion of the products, the authors were able to obtain flame front patterns that resemble the mono- and bi-cellular patterns shown in the experiments.

As a consequence of that numerical analysis, Brailovsky et al.<sup>26</sup> conjectured the existence of a kind of flameball regime travelling with a constant velocity. This regime was numerically reproduced by Grcar<sup>24</sup>, finding similarities to the prop-

agating flames shown in Fig. 1 (a) or (b). The conditions of its existence were investigated in Brailovsky et al.<sup>26</sup> utilizing a single cell in a one dimensional formulation based on a thermal diffusive model. Notably, the velocity of propagation of the flamelet shows a dependence on heat losses and activation energy.

In spite of the efforts carried out as well as the analogous similar physical phenomena which has been previously summarized, the combustion regimes discovered in Veiga-López et al.<sup>1</sup> are far from being understood. Detailed observation of the flow pattern arising in the flame fronts of Martínez-Ruiz et al.<sup>4</sup>, allows suspecting that, at least for bi-cellular cases (shown in Fig. 1 (b)), the fuel concentration mechanism involved to create hot spots is actually not diffusion, but convection. This would represent a major physical departure from the flame-ball concept as well as from the fingering in smoldering. Also, any description of the size, velocity and distance among fingers is still lacking.

Therefore, we devote this paper to obtain a first estimation of the velocity of the propagation of fingers and its size. The simplicity and applicability of the model of Brailovsky et al.<sup>26</sup> motivates its adoption, with the necessary tuning, in this investigation.

## II. MATHEMATICAL MODEL

### A. Base model and considerations

We consider the problem of a stationary isolated finger flame of width  $2R$ , in a semi-infinite horizontal Hele-Shaw cell of gas layer thickness  $2a$ , separated from the other fingers a distance  $2\ell$ , propagating at a constant speed  $V$  through a large amount of fresh gases. The oxidation reaction takes place in a planar infinitely-thin surface, which is followed by a relatively-long tail where diffusion of the combustion products and heat losses take place.

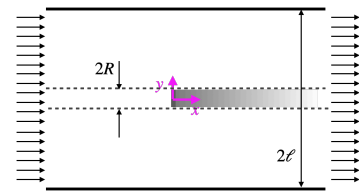


FIG. 2. Top view sketch of the finger flame, in a plane parallel to the plates of the Hele-Shaw cell, parallel itself to the plane of the paper. View from the top. The gaseous layer, of  $2a$  thickness, is perpendicular to the plane of the paper.

### 1. Formulation of the system of equations

We formulate a mathematical model considering a reference frame attached to the flame. We utilize the thermo-

diffusive model in the form adopted by Brailovsky and Sivashinsky<sup>26</sup>, based on the work of Matkovsky and Sivashinsky<sup>27</sup>. The system of equations reads

$$V \frac{\partial T}{\partial x} = \frac{\partial^2 T}{\partial x^2} + \frac{\partial^2 T}{\partial y^2} - Q(T) + (1 - \sigma) e^{\frac{1}{2}N(T-1)} \sqrt{1 + F_y^2} \delta(x - F(y)), \quad (1)$$

$$V \frac{\partial C}{\partial x} = \frac{1}{Le} \left( \frac{\partial^2 C}{\partial x^2} + \frac{\partial^2 C}{\partial y^2} \right) - e^{\frac{1}{2}N(T-1)} \sqrt{1 + F_y^2} \delta(x - F(y)). \quad (2)$$

where  $T$  is the dimensionless temperature,  $C$  is the concentration of fuel species,  $Q$  are the dimensionless heat losses,  $N$  represents the dimensionless activation temperature,  $Le = \chi/D$  is Lewis number with  $\chi$  the thermal diffusivity of the mixture and  $D$  the molecular diffusivity of the deficient fuel in the mixture,  $\delta$  is the Dirac delta function, that controls that the reaction only occurs at an infinitely-thin surface and  $\sigma$  is the dimensionless temperature of the fresh reactants (inverse of the of the expansion factor in its usual definition). The variables are made dimensionless in terms of the adiabatic temperature of the combustion products,  $T_b$ , the amount of deficient reactant (fuel) in the fresh mixture,  $C_0$ , and the thermal width of the flame  $l_{th} = \chi/S_L$  where  $S_L$  is the speed of the adiabatic flame. The system of equations (1)-(2) describes a flame with an infinitely thin reactive surface located at a surface described by function  $F(y)$ , to be considered planar in this work.

At this stage we may mention that in the thermo-diffusive approach the velocity field is decoupled from temperature and density changes. Therefore, the combustion phenomenon does not induce a change of momentum. We treat the velocity as a constant eigenvalue of the problem  $V$ , a fact that was experimentally ascertained by Kuznetsov and Grune<sup>7</sup>.

This approximation, with all its limitations, has been extensively utilized in the past<sup>26,27</sup> as it allows for an analytically treatable problem. Its usage is coherent with the early stage of the investigation of this phenomenon, in which conclusions of qualitative and approximate nature should be drawn.

The usage of the thermo-diffusive approach and the treatment of the velocity, is also supported by the thin gap between the plates of the Hele-Shaw cell. This makes  $Re$  small. For the considered dendritic flames, it remains<sup>28</sup> in the interval  $Re \in [25, 75]$ , with a low Karlovitz number  $Ka \in [0.4, 1.5]$ . According to Borghi diagram, it corresponds to flamelet wrinkled flames in a completely laminar regime.

### B. Boundary conditions

We consider a fresh mixture at  $x \rightarrow -\infty$  moving with a velocity  $V$  in the direction of the flame,

$$T = \sigma, C = 1, V = V \text{ at } x \rightarrow -\infty. \quad (3)$$

The finger is surrounded by a large amount of gases that do not burn (Fig. 2). At the narrow band of the finger indicated by

slashed lines in Fig. 2, we may formulate approximate boundary conditions to achieve a simplified one-dimensional formulation of Fig. 3. In the transverse direction conditions are the

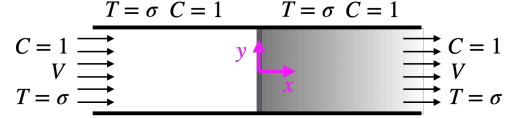


FIG. 3. Sketch of the finger flame, plane XY. Plates are parallel to the plane of the paper. View from the top. The boundary conditions are indicated upstream, downstream and in the lateral of the flame.

ones of the quiescent fresh gas outside the laterally-bounded domain,

$$T = \sigma, C = 1, V = 0 \text{ at } |y| \geq R. \quad (4)$$

Because of the diffusion of the products, at a far-enough upstream and downstream distance from the flame, the conditions of the gas are those of the fresh gases. That is, at  $x \rightarrow \pm\infty$  the gas can also be considered fresh with a velocity  $V$ ,

$$T = \sigma, C = 1, V = V \text{ at } x \rightarrow \pm\infty. \quad (5)$$

We postulate a complete consumption of the fuel at the flame,

$$C = 0 \text{ at } x = 0, y \in [-R, R]. \quad (6)$$

Heat losses are only considered in a local area around the top and bottom plates of the Hele-Shaw cell at room temperature ( $z = \pm a$ ) and take the form

$$Q = \frac{Nu}{a} (T - \sigma) \delta(z \pm a), \quad (7)$$

where  $Nu$  is the Nusselt number. Note that for fully developed flow<sup>29</sup> between plates,  $Nu \approx 8$ . This value is the absolute possible minimum.

### C. Simplifications

We carry out some simplifications to achieve a one dimensional model.

1. We consider that the reactive part of the flame is symmetric with respect to the  $y$  and  $z$  axes, flat and located at the origin. Thus  $F_y = 0$ , and  $F \equiv 0$  in  $y \in [-R, R]$ ,  $x = 0$ .
2. The fuel concentration and the temperature at the lateral limits  $y = \pm R$  are known, see (4). Therefore, we may model the lateral temperature gradient as,

$$\frac{\partial T}{\partial y} \approx -\frac{T - \sigma}{R}, \quad (8)$$

and the deficient species concentration as,

$$\frac{\partial C}{\partial y} \approx -\frac{C - 1}{R}. \quad (9)$$

We may now integrate in a quarter of the channel, apply the symmetry and divide by the transversal area  $aR$  to obtain

$$V \frac{\partial T}{\partial x} = \frac{\partial^2 T}{\partial x^2} - \frac{T - \sigma}{R^2} - \frac{Nu}{a^2} (T - \sigma) + (1 - \sigma) e^{\frac{1}{2}N(T-1)} \delta(x), \quad (10)$$

$$V \frac{\partial C}{\partial x} = \frac{1}{Le} \left( \frac{\partial^2 C}{\partial x^2} - \frac{C - 1}{R^2} \right) - e^{\frac{1}{2}N(T-1)} \delta(x). \quad (11)$$

Note that at this stage the approximation of the transversal gradients by formulae (8) and (9) and the heat losses by the equation (7) is quite arbitrary. Other models may be possible providing similarly inexact approximations. We insist on the qualitative orientation of this study. Also, if  $R$  is known,  $V$  can be interpreted as the eigenvalue of the problem.

#### D. Solution of the differential system

Following the rationale of the previous approximation, we divide the domain of interest into two areas. Out of  $x = 0$  where the exponential reaction terms of equations (10)-(11) cancel. At the flame,  $x = 0$ , we have the jump conditions included later in eqs. (16)-(18). Out of  $x = 0$ , the differential equations are second order, linear and homogeneous. Following<sup>30</sup> the generic equation

$$y'' - ay' - by + c = 0, \quad (12)$$

with constant coefficients,  $a, b, c$  has solutions of the form

$$y = K_1 \exp \left[ \left( \frac{a}{2} - \sqrt{\left( \frac{a}{2} \right)^2 + b} \right) x \right] + K_2 \exp \left[ \left( \frac{a}{2} + \sqrt{\left( \frac{a}{2} \right)^2 + b} \right) x \right] + \frac{c}{b}, \quad (13)$$

where  $K_1$  and  $K_2$  are constants to be determined. Note that contrary to the original formulation of Brailovsky et al.<sup>26</sup> we disregard radiation losses. Therefore, we directly obtain linear differential equations, a fact that allows for a simpler mathematical treatment than in the reference.

Considering the continuity of the variables at  $x = 0$  and that in  $x \rightarrow \pm\infty$  the variables must remain finite, it is immediate to obtain,

$$T^\pm = T_f \exp \left( \left[ \frac{V}{2} \mp \sqrt{\left( \frac{V}{2} \right)^2 + \frac{1}{R^2} + \frac{Nu}{a^2}} \right] x \right) + \sigma, \quad (14)$$

$$C^\pm = -\exp \left( \left[ \frac{VLe}{2} \mp \sqrt{\left( \frac{VLe}{2} \right)^2 + \frac{1}{R^2}} \right] x \right) + 1. \quad (15)$$

This system has three unknown parameters, the temperature at the flame,  $T_f$ , the flame velocity,  $V$ , and the thickness of the finger,  $R$ . A generic solution of this system is shown in Figure 4.

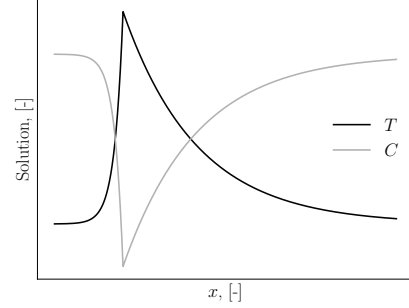


FIG. 4. Generic solution of equations (14) and (15).

#### E. Solution of the system

The previous equations offer a clear way to divide the domain of interest into separate areas. Out of  $x = 0$  the exponential term of the equations cancel. On the contrary, at  $x = 0$  and  $y \in [-R, R]$  we have

$$[\theta] = [C] = 0, \quad (16)$$

$$\left[ \frac{\partial \theta}{\partial x} \right] = -R^2 W, \quad (17)$$

$$\left[ \frac{\partial C}{\partial x} \right] = R^2 Le W, \quad (18)$$

where the Arrhenius term,  $W = e^{\frac{1}{2}N(T_f-1)}$ .

##### 1. General case

We may introduce equations (14) and (15) in the conditions (17)-(18). Immediately we obtain,

$$2\sqrt{\left( \frac{V}{2} \right)^2 + \frac{1}{R^2} + \frac{Nu}{a^2}} T_f = (1 - \sigma) e^{\frac{1}{2}N(T_f-1)}, \quad (19)$$

$$2\sqrt{\left( \frac{VLe}{2} \right)^2 + \frac{1}{R^2}} = Le e^{\frac{1}{2}N(T_f-1)}. \quad (20)$$

We can now solve  $T_f$ ,

$$T_f = \frac{1 - \sigma}{Le} \frac{\sqrt{\left( \frac{VLe}{2} \right)^2 + \frac{1}{R^2}}}{\sqrt{\left( \frac{V}{2} \right)^2 + \frac{1}{R^2} + \frac{Nu}{a^2}}}. \quad (21)$$

Taking this result into equation (20), we obtain

$$2\sqrt{\left(\frac{VLe}{2}\right)^2 + \frac{1}{R^2}} = Le \exp\left(\frac{1}{2}N \left[ \frac{1-\sigma}{Le} \frac{\sqrt{\left(\frac{VLe}{2}\right)^2 + \frac{1}{R^2}}}{\sqrt{\left(\frac{V}{2}\right)^2 + \frac{1}{R^2} + \frac{Nu}{a^2}}} - 1 \right]\right), \quad (22)$$

a relation between the thickness of the finger and its velocity given a certain amount of heat losses, Lewis number  $Le$ , density jump  $\sigma$  and activation energy  $N$ .

We depict equation (22) particularized for  $Nu = 8$ ,  $Le = 0.25$  and  $\sigma = 0.33$  in Figures 5 and 6 given  $N = 8$  and  $N = 60$  respectively, which are values close to those obtained for lean hydrogen flames with  $\phi \approx 0.195$ . The lower limit of  $R = 5$  was selected to fairly reproduce characteristic flame sizes reported in the experiments. We believe that for flames widths close to the flame thickness,  $R \rightarrow 1$ , the results are not of practical interest.

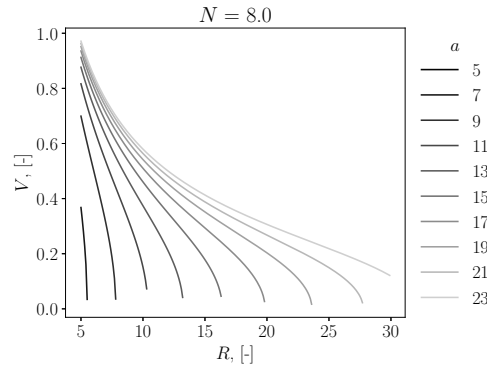


FIG. 5. Flame speed as a function of the flame radius for varying channel thickness  $a$  and activation energy  $N = 8$ .

We observe that the maximum radius  $R$  appears when the flame propagates slowly, that is,  $V \rightarrow 0$ , which happens to be similar to the thickness of the channel,  $a$ . The fastest velocities are obtained when  $R \rightarrow 5$ , being these faster for increasing values of  $a$  because heat losses weaken. Given  $a > 8$  and  $N = 60$ , the maximum velocities within the selected range of  $R$  are higher than the laminar burning velocity of the mixture. Diffusion ( $Le < 1$ ) increases the fuel presence at the reaction area, thus increasing the local equivalence ratio and speeding up the flame. In addition, for higher activation energies, the maximum expected size of the flames reduces from  $R \approx 30$  with  $N = 8$  to  $R \approx 20$  with  $N = 60$ , which can be directly related to a decrease in flammability.

With the values obtained for  $V$  and  $R$ , the temperature  $T_f$  was obtained using equation (21). The results are shown in

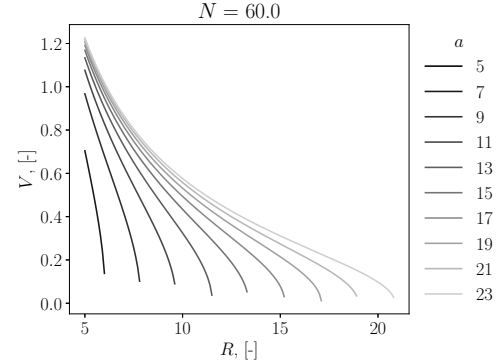


FIG. 6. Flame speed as a function of the flame radius for varying channel thickness  $a$  and activation energy  $N = 60$ .

Figs. 7 and 8 for  $N = 8$  and  $N = 60$  respectively. A decrease of  $a$  induces a reduction of the minimal allowable temperature, directly related to the increase of heat losses. Likewise, small  $a$  means overheating, whilst for larger  $a$  allowable solutions involve both over and under heating. Regardless of  $a$ , the flames are overheated when  $R < 10$ . Note that for increasing values of the dimensionless activation energy  $N$ , the flame temperature always stays around the adiabatic value.

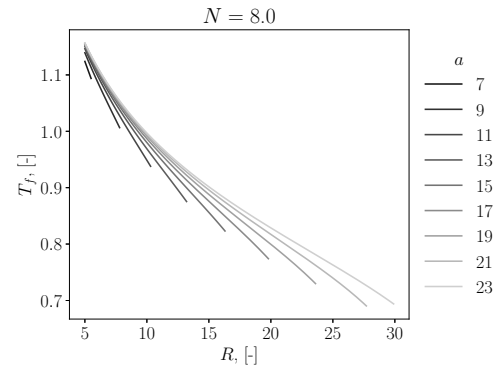


FIG. 7. Temperature values as a function of the flame radius for varying channel thickness  $a$  and activation energy  $N = 8$ .

## 2. The limit $N \rightarrow \infty$

Equation (22) can be approximated for a single solution in those cases in which the approximation  $N \rightarrow \infty$  is reasonable. In order for (22) to be valid, it must happen that the terms under square brackets cancel. If it would be positive the exponential term will tend to infinity. If it would be negative,

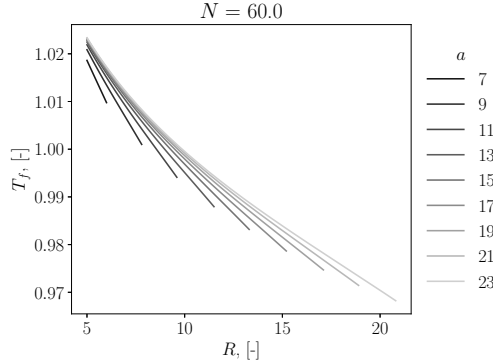


FIG. 8. Temperature values as a function of the flame radius for varying channel thickness  $a$  and activation energy  $N = 60$ .

$(VLe/2)^2 = -1/R^2$ , which is absurd. Thus,

$$2\sqrt{\left(\frac{VLe}{2}\right)^2 + \frac{1}{R^2}} = Le, \quad (23)$$

$$\frac{1-\sigma}{Le} \frac{\sqrt{\left(\frac{VLe}{2}\right)^2 + \frac{1}{R^2}}}{\sqrt{\left(\frac{V}{2}\right)^2 + \frac{1}{R^2} + \frac{Nu}{a^2}}} = 1. \quad (24)$$

Rearranging this system and rewriting it in terms of  $(V/2)^2$  and  $1/R^2$  we obtain,

$$Le^2 \left(\frac{V}{2}\right)^2 + \frac{1}{R^2} = \frac{Le^2}{4}, \quad (25)$$

$$-(1-(1-\sigma^2)) \left(\frac{V}{2}\right)^2 + \left(\frac{(1-\sigma)^2}{Le^2} - 1\right) \frac{1}{R^2} = \frac{Nu}{a^2}. \quad (26)$$

For the second equation to remain valid the following condition holds,

$$Le < 1 - \sigma. \quad (27)$$

Constrain (27) does not contradict the findings of Yanez et al.<sup>2</sup> relative to the heat losses as a triggering factor of the unconventional propagation. Note that  $Le$  is almost constant for a large range of lean  $H_2$ -air mixtures, and  $\sigma$  decreases with the concentration of hydrogen. That is, condition (27) is fulfilled for lean mixtures. Unconventional regimes were not reported for rich-enough mixtures ( $\% H_2 > 20$ ).

Equation (27) is very important to exclude the possible existence of unconventional flame propagation regimes for rich mixtures, characterized by  $Le > 1$ . At rich conditions, a conjectured mechanism for the existence of finger flames can be similar to the one described by<sup>9</sup> and<sup>17</sup>. That is, oxygen

diffusing through nitrogen and hydrogen in the direction of the flame front. That mechanism, is now excluded by condition (27), confirming the findings of Martínez-Ruiz et al.<sup>4</sup> which were not able to numerically reproduce unconventional regimes for very rich mixtures.

Solving the system we obtain,

$$\frac{1}{R^2} = Le^2 \frac{\frac{1}{4}(1-(1-\sigma)^2) + \frac{Nu}{a^2}}{1 - Le^2}, \quad (28)$$

$$\left(\frac{V}{2}\right)^2 = \frac{1}{1 - Le^2} \left[ \frac{(1-\sigma)^2 - Le^2}{4} - \frac{Nu}{a^2} \right]. \quad (29)$$

Equations (28) and (29) are shown in Figures 9 and 10 particularized for  $Nu = 8$ ,  $Le = 1/4$  and  $\sigma = 1/3$ . The velocity and radius of the propagating flame balls increases for increasing gap thickness  $a$ , as heat losses through the walls diminish. The radius of the flame will be approximately of the same order than the gap size. Regarding the propagation flame speed, heat losses slow down the flame, impeding its complete acceleration towards  $V \rightarrow 1$ .

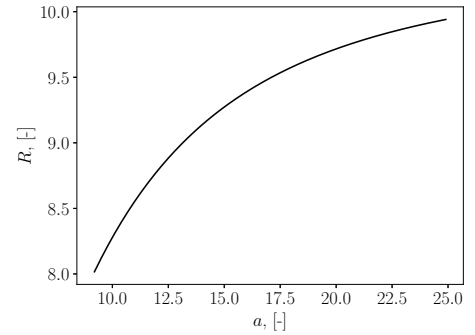


FIG. 9. Flame size as a function of the gap thickness given  $N \rightarrow \infty$ .

### 3. Comparison with experimental findings

We compare previous results with the measurements of Veiga-López et al.<sup>1</sup>. The single-headed case (Fig. 1-a) had experimental conditions  $2\tilde{a} = 3$  mm,  $\phi = 0.195$  and  $\tilde{S}_L \approx 5.4$  cm/s, where *tilde* indicates dimensional magnitudes. Measured from the videos, the propagating speed of the finger flames was around  $\tilde{V} = 11$  cm/s. It doubled the laminar burning velocity. On the contrary, our model gives  $\tilde{V}_{\text{model}} = 2.7$  cm/s, half of  $\tilde{S}_L$ . The flame width is  $2\tilde{R} = 4$  mm, of the same order as  $2\tilde{a}$  as assessed by our reduced model.

This divergence can be justified considering the departure in the conditions among the experiments and the model. The flames propagate vertically in the experiments, with gravity effecting significantly their dynamics, whilst this effect is disregarded in the construct.



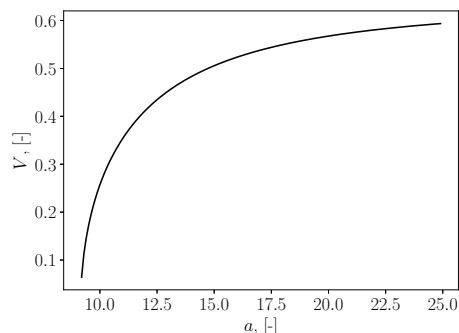


FIG. 10. Flame speed as a function of the gap thickness given  $N \rightarrow \infty$ .

An estimation of the gravity effect may be carried out neglecting viscosity (Rayleigh number  $Ra \ll 1$ ) and heat losses. An overestimation of the velocity due to buoyancy,  $\tilde{V}_g = \sqrt{(1 - \bar{\rho}_b/\bar{\rho}_0) g 2a} \approx 13 \text{ cm/s}$ , is obtained. The mixture densities before ( $\bar{\rho}_0$ ) and after ( $\bar{\rho}_b$ ) the chemical reaction were obtained using Cantera<sup>31</sup> and the San Diego mechanism for hydrogen<sup>32</sup>, whilst  $g$  represents the constant of gravity.  $\tilde{V}_g$  is higher than the adiabatic flame velocity, thus buoyancy effects are, at least, as important as flame propagation ( $\tilde{S}_L$ ). This reason does not allow us to compare the model and the experimental case, as the reported values for the latter are masked by buoyancy.

### III. CONCLUSIONS

A simple one-dimensional model for steady finger-like flames is reported in this work. The construct was created using a thermo-diffusive model<sup>27, 26</sup>. The proposed formulation can be applied to a stationary non-splitting isolated finger flame, far away from the next finger. It allows for the calculation of the flame velocity, temperature, and flamelet size, as a function of the thickness of the Hele-Shaw cell, the expansion rate, activation energy and Lewis number.

In addition, under the assumption of infinite Zel'dovich number ( $N \rightarrow \infty$ ), a second and simpler approximation is obtained for the temperature, velocity and size of a finger flame. Under such assumption, it is concluded that rich hydrogen flames and other mixtures characterized by  $Le \geq 1$  cannot exhibit such a phenomenon.

To the best of our knowledge, the proposed formulation constitutes the first attempt to provide mathematical expressions that characterize the phenomena at hand. Nevertheless, the research in the topic is far from being completed.

Notably, the construct does not include the effect of buoyancy. This effect appears to be of particular importance for the phenomenon. This impacts twofold, both for experiments and for theory. First, an improvement of the model includ-

ing this effect is necessary. Second, additional experiments isolating dendritic gaseous combustion from buoyancy (horizontally propagating flames) may be beneficial for the understanding of the phenomenon.

Flame curvature may be an additional source of discrepancy between the model and the experiments. In seek of simplicity, the model considers a planar flame front. The experimental images of<sup>1</sup> as well as the calculations of<sup>4</sup> show a significantly curved front in the plane of the Hele-Shaw cell. The curvature of the front may create local hot spots, increase the surface-to-volume ratio, and induce lateral velocity gradients. Therefore, flame curvature may affect the flame propagation velocity, influence the maximum allowable heat losses, and originate the regime shown in Fig. 1-b.

Future works in this topic will include curvature and buoyancy in the model and extend the formulation to 2D.

### ACKNOWLEDGMENTS

We wish to thank Prof. Sivashinsky for the interesting discussion on<sup>26</sup>. We also acknowledge Dr. Kourdioumov for his comments on the preliminary version of this analysis.

<sup>1</sup>F. Veiga-López, M. Kuznetsov, D. Martínez-Ruiz, E. Fernández-Tarrazo, J. Grune, and M. Sánchez-Sanz, "Unexpected propagation of ultra-lean hydrogen flames in narrow gaps," *Physical review letters* **124**, 174501 (2020).

<sup>2</sup>J. Y. Escanciano, M. Kuznetsov, and F. Veiga-López, "Characterization of unconventional hydrogen flame propagation in narrow gaps," *Physical Review E* **103**, 033101 (2021).

<sup>3</sup>F. Veiga López, "Flame propagation in narrow channels," (2020).

<sup>4</sup>D. Martínez-Ruiz, F. Veiga-López, D. Fernández-Galisteo, V. N. Kurdyumov, and M. Sánchez-Sanz, "The role of conductive heat losses on the formation of isolated flame cells in hele-shaw chambers," *Combustion and Flame* **209**, 187–199 (2019).

<sup>5</sup>A. Domínguez-González, D. Martínez-Ruiz, and M. Sánchez-Sanz, "Stable circular and double-cell lean hydrogen-air premixed flames in quasi two-dimensional channels," *Proceedings of the Combustion Institute* (2022).

<sup>6</sup>L. Kagan and G. Sivashinsky, "Pattern formation in flame spread over thin solid fuels," *Combustion Theory and Modelling* **12**, 269–281 (2008).

<sup>7</sup>M. Kuznetsov and J. Grune, "Experiments on combustion regimes for hydrogen/air mixtures in a thin layer geometry," *International Journal of Hydrogen Energy* **44**, 8727–8742 (2019).

<sup>8</sup>Y. Zhang, P. Ronney, E. Roegner, and J. Greenberg, "Lewis number effects on flame spreading over thin solid fuels," *Combustion and flame* **90**, 71–83 (1992).

<sup>9</sup>O. Zik, Z. Olami, and E. Moses, "Fingering instability in combustion," *Physical review letters* **81**, 3868 (1998).

<sup>10</sup>O. Zik and E. Moses, "Fingering instability in combustion: an extended view," *Physical Review E* **60**, 518 (1999).

<sup>11</sup>T. Matsuoka, K. Nakashima, Y. Nakamura, and S. Noda, "Appearance of flamelets spreading over thermally thick fuel," *Proceedings of the Combustion Institute* **36**, 3019–3026 (2017).

<sup>12</sup>F. Zhu, Z. Lu, S. Wang, and Y. Yin, "Microgravity diffusion flame spread over a thick solid in step-changed low-velocity opposed flows," *Combustion and Flame* **205**, 55–67 (2019).

<sup>13</sup>J. Malchi, R. Yetter, S. Son, and G. Risha, "Nano-aluminum flame spread with fingering combustion instabilities," *Proceedings of the Combustion Institute* **31**, 2617–2624 (2007).

<sup>14</sup>S. Olson, H. Baum, and T. Kashiwagi, "Finger-like smoldering over thin cellulosic sheets in microgravity," in *Symposium (International) on Combustion*, Vol. 27 (Elsevier, 1998) pp. 2525–2533.

<sup>15</sup>G. I. Sivashinsky, "Nonlinear analysis of hydrodynamic instability in laminar flames—i. derivation of basic equations," *Acta astronautica* **4**, 1177–1206 (1977).

This is the author's peer reviewed, accepted manuscript. However, the online version of record will be different from this version once it has been copyedited and typeset.

PLEASE CITE THIS ARTICLE AS DOI: 10.1063/5.0118271

Accepted to Phys. Fluids 10.1063/5.0118271

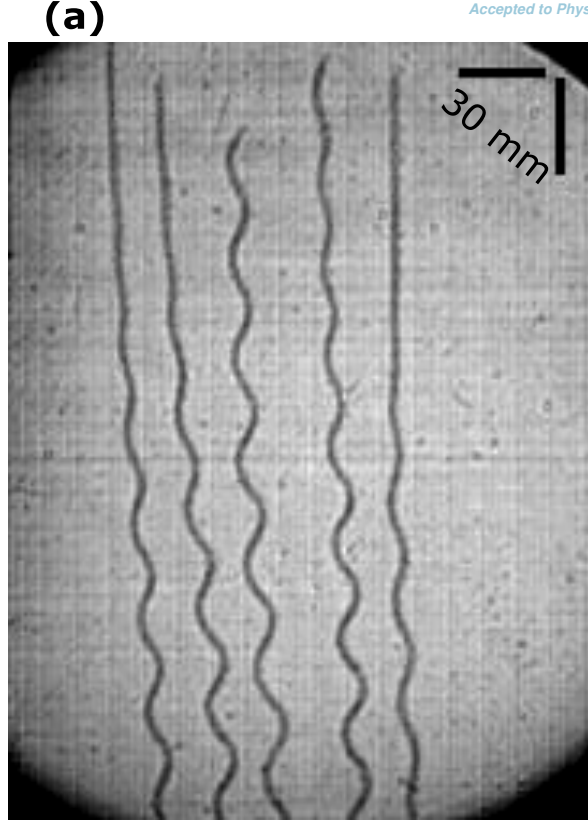
8

- <sup>16</sup>P. D. Ronney, "Understanding combustion processes through microgravity research," in *Symposium (International) on Combustion*, Vol. 27 (Elsevier, 1998) pp. 2485–2506.
- <sup>17</sup>P. D. Ronney, "Near-limit flame structures at low lewis number," *Combustion and Flame* **82**, 1–14 (1990).
- <sup>18</sup>P. D. Ronney, M.-S. Wu, H. G. Pearlman, and K. J. Weiland, "Experimental study of flame balls in space: Preliminary results from sts-83," *AIAA journal* **36**, 1361–1368 (1998).
- <sup>19</sup>J. Buckmaster, G. Joulin, and P. Ronney, "The structure and stability of nonadiabatic flame balls," *Combustion and Flame* **79**, 381–392 (1990).
- <sup>20</sup>J. Buckmaster, G. Joulin, and P. Ronney, "The structure and stability of nonadiabatic flame balls: II. effects of far-field losses," *Combustion and Flame* **84**, 411–422 (1991).
- <sup>21</sup>J. Buckmaster, M. Smooke, and V. Giovangigli, "Analytical and numerical modeling of flame-balls in hydrogen-air mixtures," *Combustion and Flame* **94**, 113–124 (1993).
- <sup>22</sup>J. Buckmaster and G. Joulin, "Flame balls stabilized by suspension in fluid with a steady linear ambient velocity distribution," *Journal of fluid mechanics* **227**, 407–427 (1991).
- <sup>23</sup>J. Buckmaster, "Influence of boundary-induced losses on the structure and dynamics of flame-balls," *Combustion Science and Technology* **89**:1–4, 57–69 (1993).
- <sup>24</sup>J. F. Grcar, "A new type of steady and stable, laminar, premixed flame in ultra-lean, hydrogen–air combustion," *Proceedings of the Combustion Institute* **32**, 1011–1018 (2009).
- <sup>25</sup>L. Kagan and G. Sivashinsky, "Self-fragmentation of nonadiabatic cellular flames," *Combustion and flame* **108**, 220–226 (1997).
- <sup>26</sup>I. Brailovsky and G. Sivashinsky, "On stationary and travelling flame balls," *Combustion and Flame* **110**, 524–529 (1997).
- <sup>27</sup>B. Matkowsky and G. Sivashinsky, "An asymptotic derivation of two models in flame theory associated with the constant density approximation," *SIAM Journal on Applied Mathematics* **37**, 686–699 (1979).
- <sup>28</sup>M. Kuznetsov, J. Yanez, and F. Veiga-López, "Near limit flame propagation in a thin layer geometry at low peclet numbers," in *Proceedings of the Eighteenth International Conference on Flow Dynamics* (2021) pp. 688–692.
- <sup>29</sup>A. Bejan and A. D. Kraus, *Heat transfer handbook*, Vol. 1 (John Wiley & Sons, 2003).
- <sup>30</sup>E. A. Coddington, *An introduction to ordinary differential equations* (Dover publishers, 1989).
- <sup>31</sup>D. G. Goodwin, R. L. Speth, H. K. Moffat, and B. W. Weber, "Cantera: An object-oriented software toolkit for chemical kinetics, thermodynamics, and transport processes," <https://www.cantera.org> (2021), version 2.5.1.
- <sup>32</sup>"Chemical-kinetic mechanisms for combustion applications," <https://web.eng.ucsd.edu/mae/groups/\combustion/mechanism.html>.

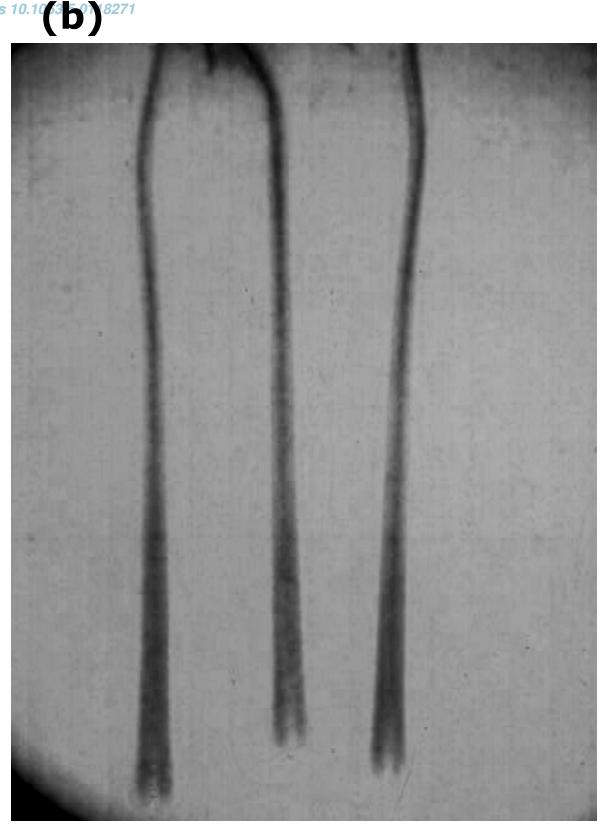


This is the author's peer reviewed, accepted manuscript. However, the online version of record will be different from this version once it has been copyedited and typeset.

PLEASE CITE THIS ARTICLE AS DOI: 10.1063/5.0118271

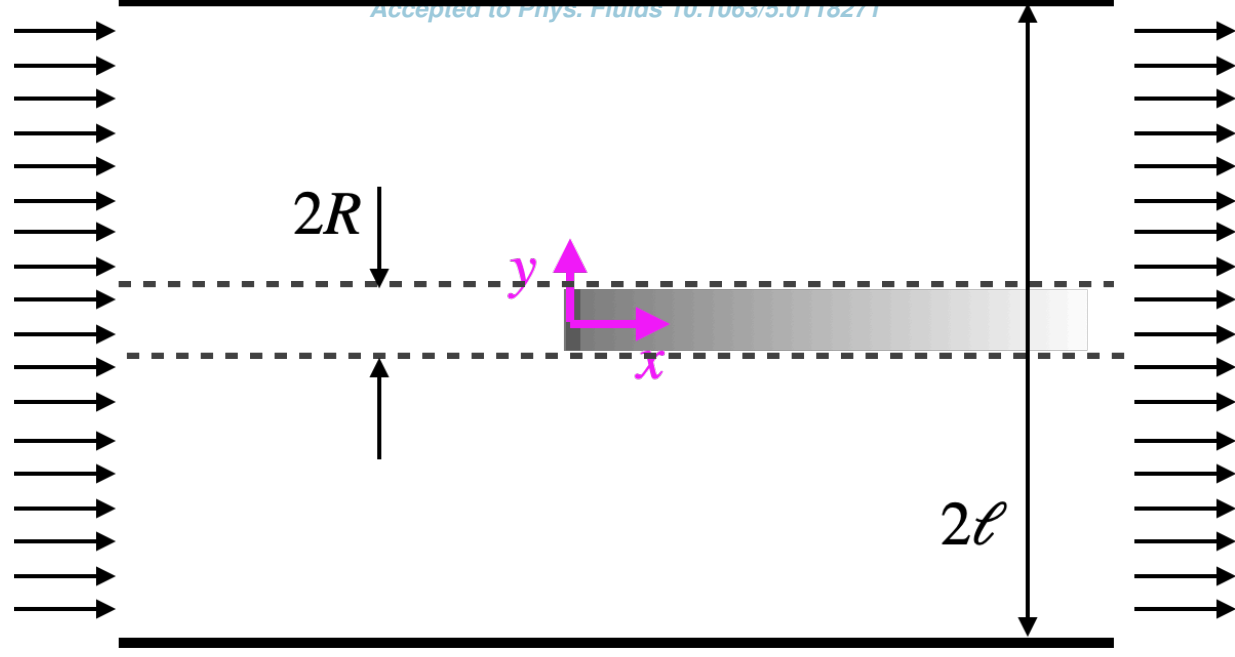


Accepted to Phys. Fluids 10.1063/5.0118271



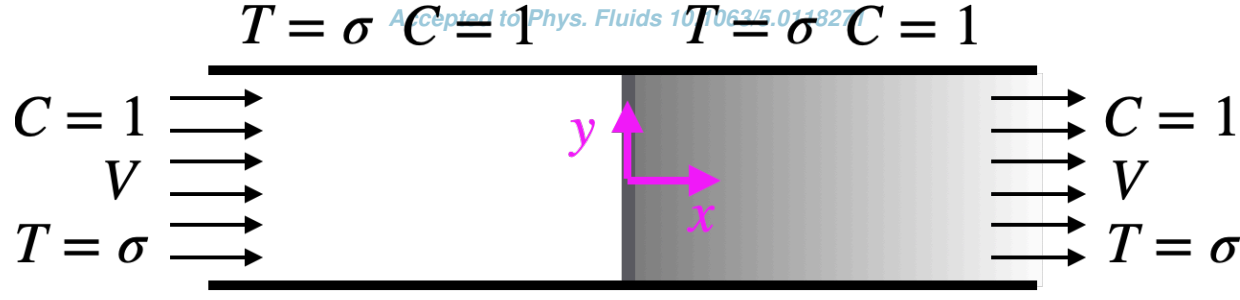
This is the author's peer reviewed, accepted manuscript. However, the online version of record will be different from this version once it has been copyedited and typeset.

PLEASE CITE THIS ARTICLE AS DOI: 10.1063/5.0118271



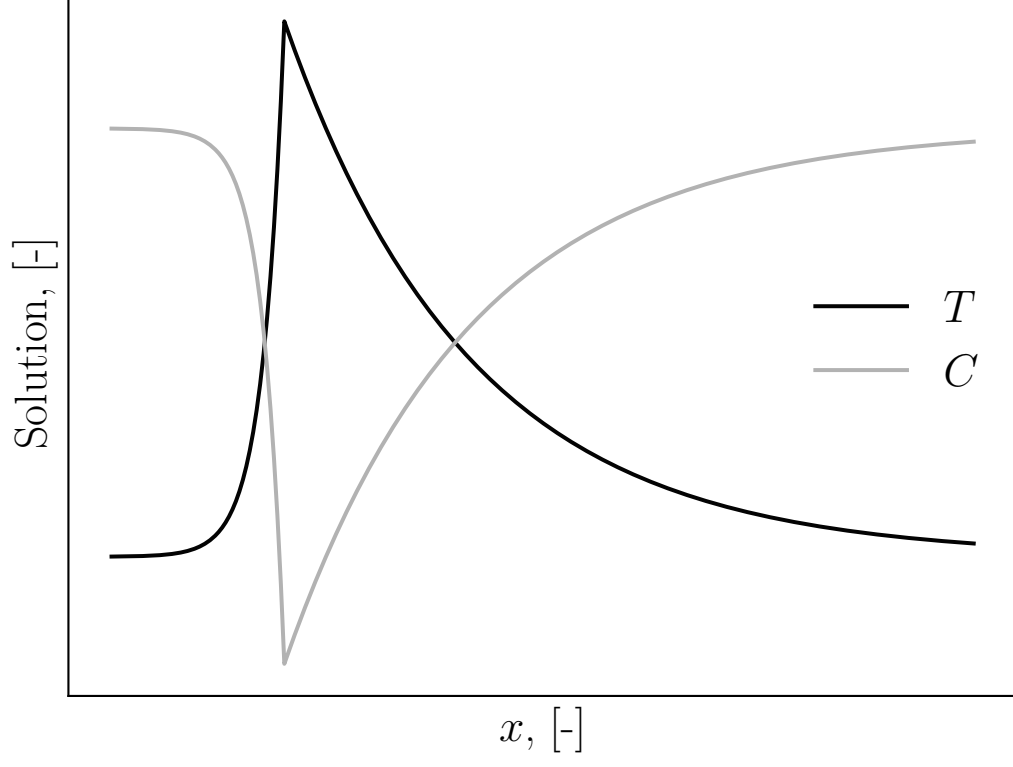
This is the author's peer reviewed, accepted manuscript. However, the online version of record will be different from this version once it has been copyedited and typeset.

PLEASE CITE THIS ARTICLE AS DOI: 10.1063/5.0118271



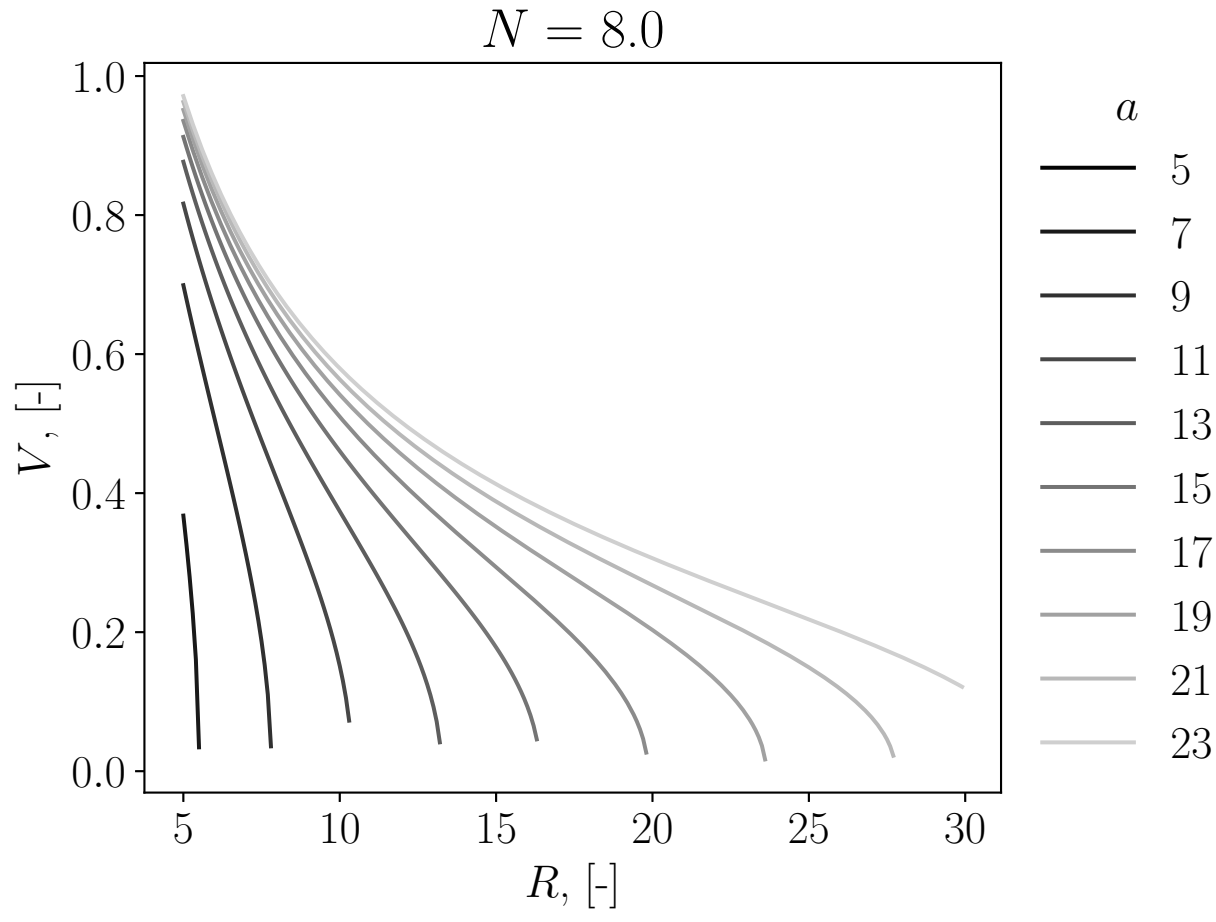
This is the author's peer reviewed, accepted manuscript. However, the online version of record will be different from this version once it has been copyedited and typeset.

PLEASE CITE THIS ARTICLE AS DOI: 10.1063/5.0118271



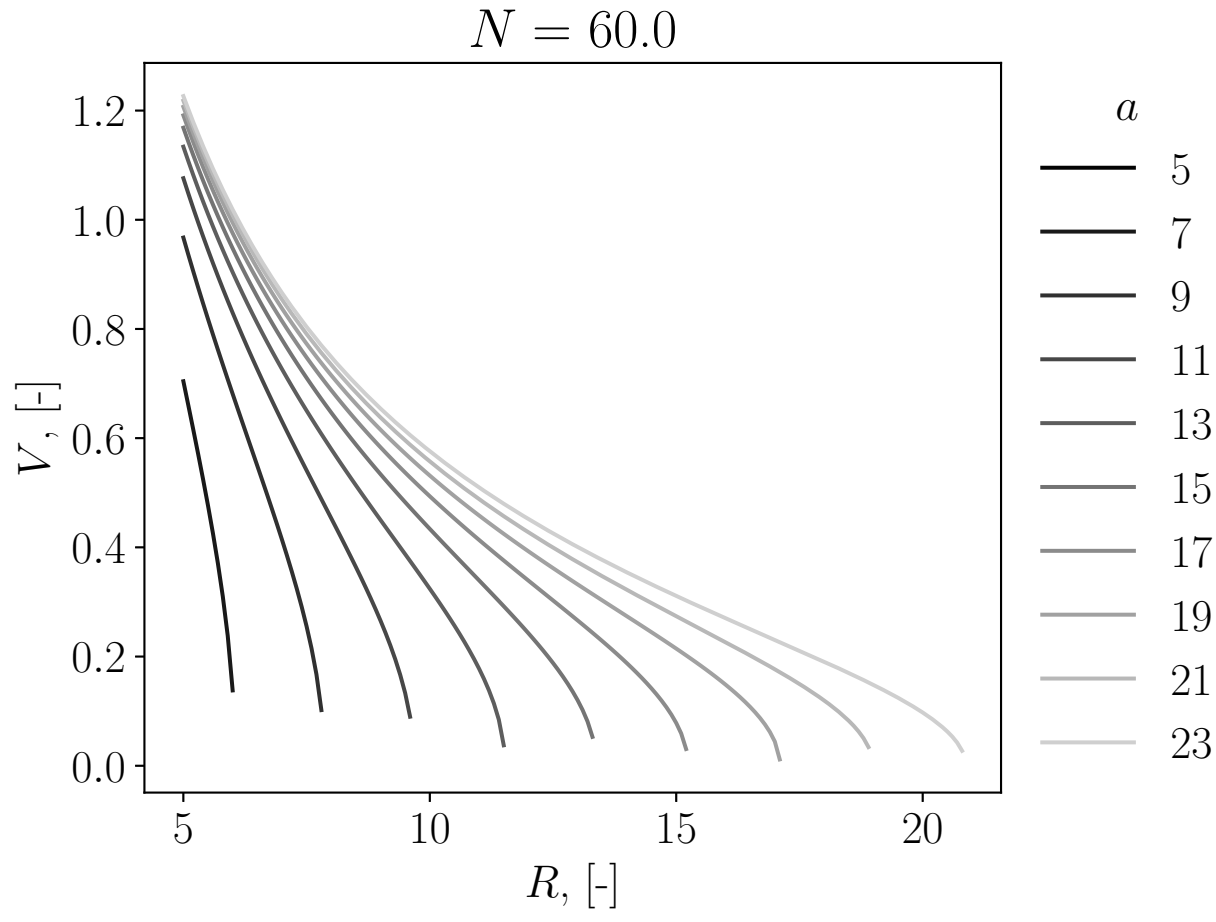
This is the author's peer reviewed, accepted manuscript. However, the online version of record will be different from this version once it has been copyedited and typeset.

PLEASE CITE THIS ARTICLE AS DOI: 10.1063/5.0118271



This is the author's peer reviewed, accepted manuscript. However, the online version of record will be different from this version once it has been copyedited and typeset.

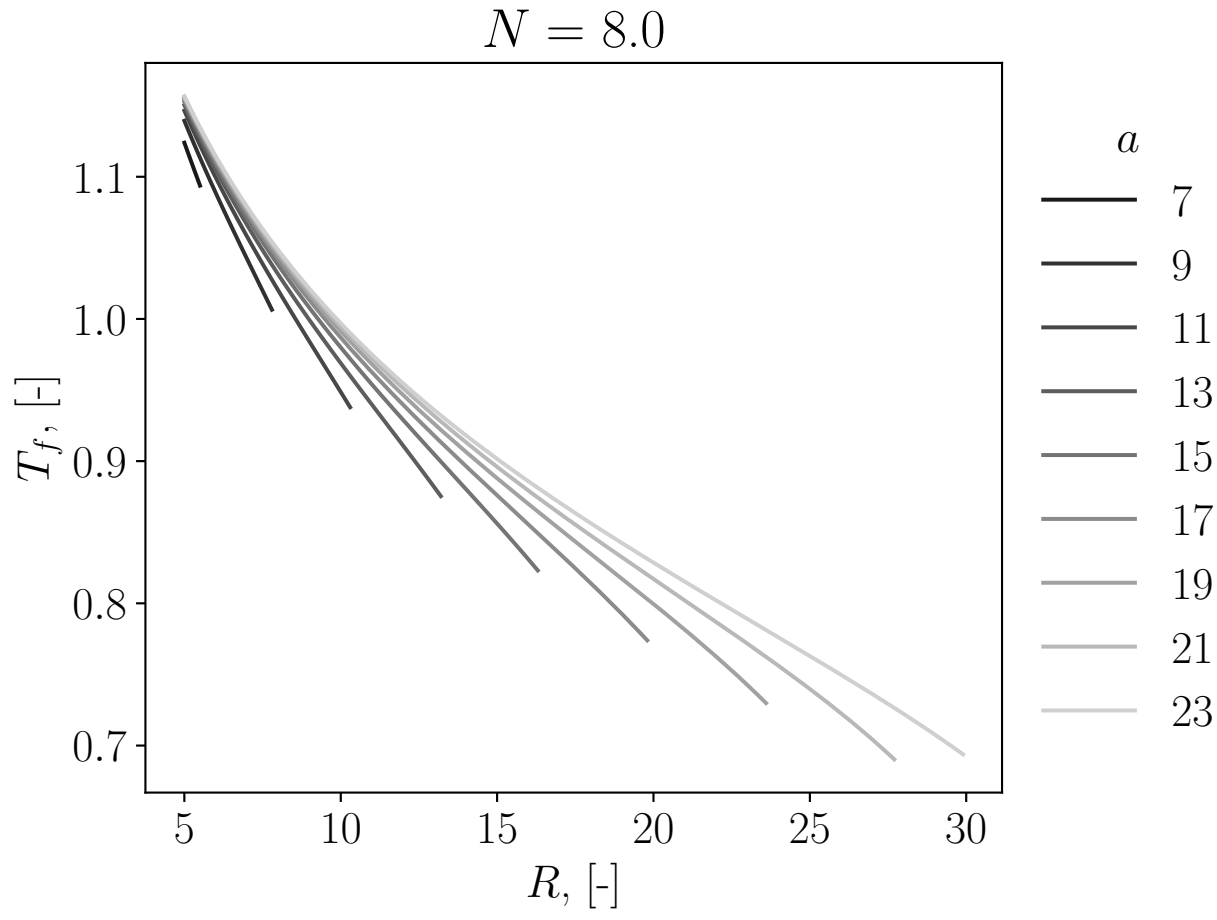
PLEASE CITE THIS ARTICLE AS DOI: 10.1063/5.0118271





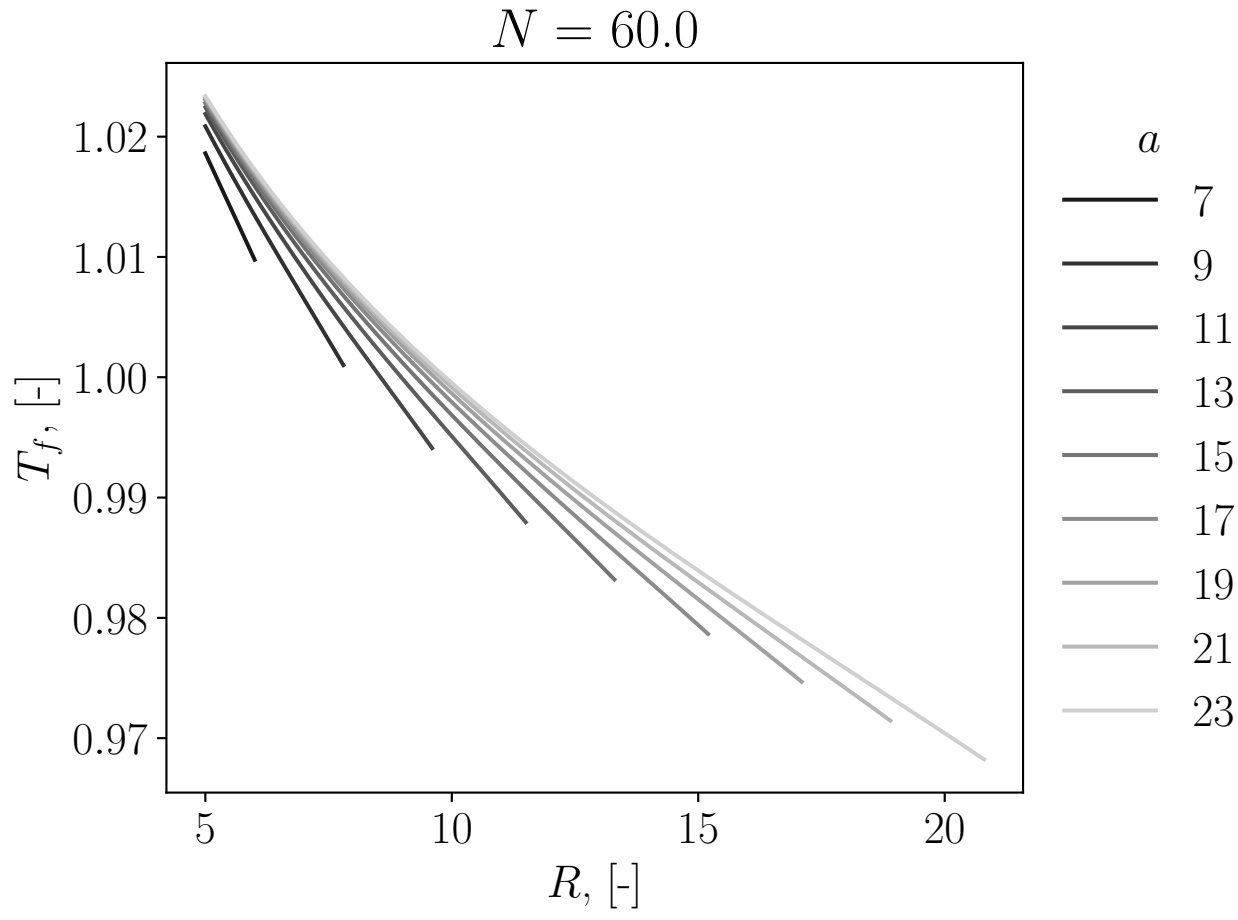
This is the author's peer reviewed, accepted manuscript. However, the online version of record will be different from this version once it has been copyedited and typeset.

PLEASE CITE THIS ARTICLE AS DOI: 10.1063/5.0118271



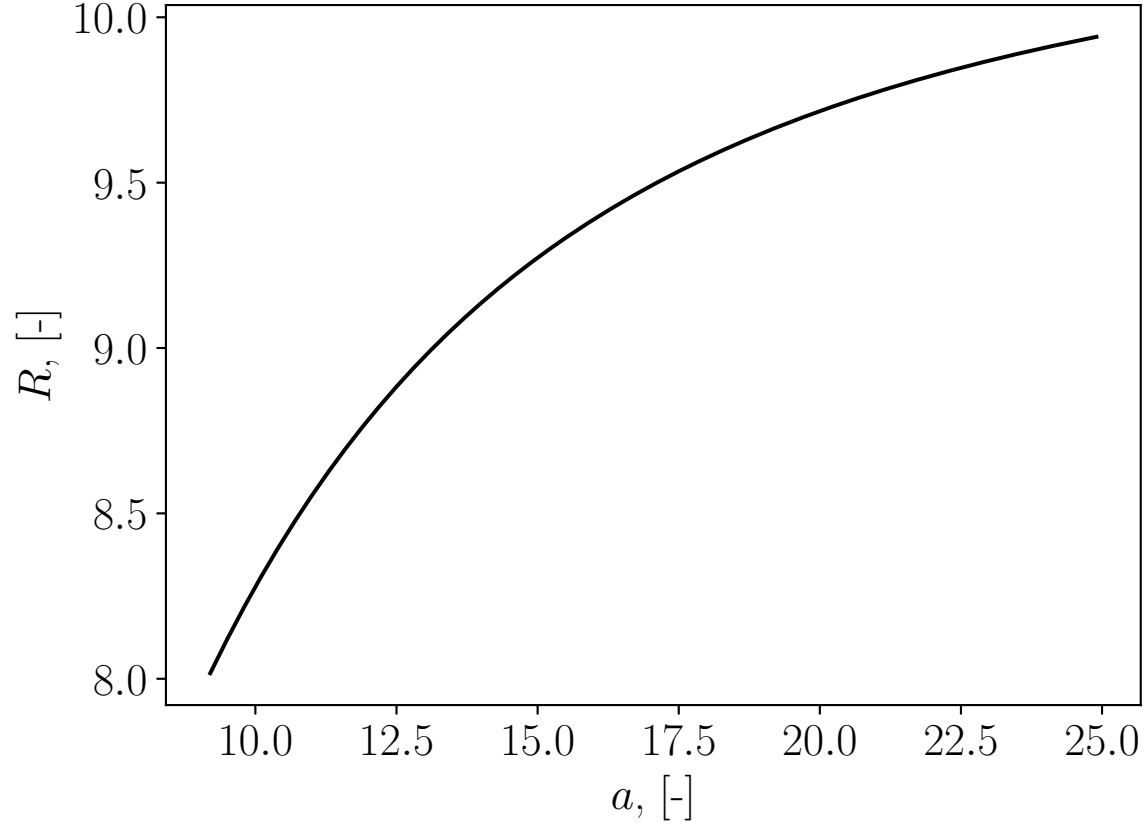
This is the author's peer reviewed, accepted manuscript. However, the online version of record will be different from this version once it has been copyedited and typeset.

PLEASE CITE THIS ARTICLE AS DOI: 10.1063/5.0118271



This is the author's peer reviewed, accepted manuscript. However, the online version of record will be different from this version once it has been copyedited and typeset.

PLEASE CITE THIS ARTICLE AS DOI: 10.1063/5.0118271



This is the author's peer reviewed, accepted manuscript. However, the online version of record will be different from this version once it has been copyedited and typeset.

PLEASE CITE THIS ARTICLE AS DOI: 10.1063/5.0118271

